ORIGINAL ARTICLE

Mathematical modeling and analysis of Covid-19 infection spreads with restricted optimal treatment of disease incidence

D. Pal[1,*], D. Ghosh[2], P.K. Santra[3], G.S. Mahapatra[2]

[1]Chandrahati Dilip Kumar High School (H.S.)
Chandrahati 712504, West Bengal, India

[2]Department of Mathematics, National Institute of Technology Puducherry
Karaikal-609609, India

[3]Maulana Abul Kalam Azad University of Technology
Kolkata-700064, India

*Correspondence email: pal.debkumar@gmail.com

Abstract— This paper presents the current situation and how to minimize its effect in India through a mathematical model of infectious Coronavirus disease (COVID-19). This model consists of six compartments to population classes consisting of susceptible, exposed, home quarantined, government quarantined, infected individuals in treatment, and recovered class. The basic reproduction number is calculated, and the stabilities of the proposed model at the disease-free equilibrium and endemic equilibrium are observed. The next crucial treatment control of the Covid-19 epidemic model is presented in India's situation. An objective function is considered by incorporating the optimal infected individuals and the cost of necessary treatment. Finally, optimal control is achieved that minimizes our anticipated objective function. Numerical observations are presented utilizing MATLAB software to demonstrate the consistency of present-day representation from a realistic standpoint.

I. INTRODUCTION

Recently, the coronavirus disease has turned out to be a pandemic over almost the whole world. The basic indication of this infection is ordinary fever, cough, and breathing problems. This virus also showed the capability to produce serious health problems among a specific group of individuals, including the aged populace as well as patients with cardiovascular disease and diabetes [1]. However, a clear picture of the nature of this

epidemiology is still being explained [2].

This virus transmits from human to human as a result, Covid-19 disease spread across the globe, and the total number of active Covid-19 cases increases day by day ([3]-[10]). In particular, India has become the stiffest affected country with Covid-19 endemic [11] due to its very high population densities. The figure for positive Covid-19 infection started to increase from 4th March 2020. As of 8th May 2020, a total of 59690 confirmed COVID cases, together with 17887 recovered and 1986 deaths in India [12]. Different precaution measures ([13]-[16]) have been taken by the Indian Government to maintain social distance [17] among the huge numbers of the population in India. There is no specific medicine for Covid-19 infection to date. Therefore, doctors recommended different treatments via medication to COVID-19 patients depending on their symptoms. The therapy and vaccine yet to get, spread of Coved 19 diseases can be restricted via appropriate precautionary measures like quarantined mechanisms ([18]-[20]), individual safeguard from the infected individual by using social distancing [21], etc. As the Covid-19 virus spread very quickly throughout the world, so various mathematical models depending on the pandemic outbreak ([22]-[32], [33], [34], [35]) have been performed already. Wu et al. [36] studied the dynamics behind the spread of Covid-19 virus world-wise using SEIR model. Read et al. [37] developed a Covid-19 SEIR model based on Poisson-distributed daily time augmentations. Paul et al. [38] presented a mathematical model on Covid-19 incorporating the different safety strategies to protect the citizens from the virus. Sardar et al. [39] proposed a mathematical model to identify the lockdown effect of the spreading of Covid-19 disease in India. Pal et al. [40] explored a Covid-19 based SEQIR model to understand India's disease situation.

This paper introduces a six-compartmental Covid-19 infection model by separating the total populace into six classes, purposely susceptible, exposed, home quarantined, government quarantined, infected individuals in treatment as well as recovered class. We introduce treatment control in the model to assimilate realistic and biologically significant in the pandemic situation. A brief description of the necessary and sufficient conditions for the existence of multi-objective optimal control is provided in Section 2. The model derivation and preliminaries are explained in Section 3. The basic properties of our proposed model structure are discussed in Section 4. In section 5, we introduce the concept of the basic reproduction number (R_0) [41]. Next, we deal with disease-free equilibrium (DFE) (E_0) and endemic equilibrium (E_1) points of the system. It is clear that Covid-19 infection is not only community health trouble [42] but also a tremendous societal and monetary shock on the developing countries. Therefore, it is an essential concern to control ([43]-[46]) the spread of Covid-19 infection in India by adopting several optimal control policies. In Section 6, we have formulated the Covid-19 epidemic model with control treatment. This section provides us a procedure to find optimal control [47] $u(t)$ that increases the recovery rate as well as minimizes the cost associated with the treatment. Analytical results are obtained in the previous sections are numerically verified in Section 7 with the help of realistic values of the model parameters using MATLAB. Lastly, a general conclusion about our proposed model structure is provided in Section 8.

II. Multi-objective optimal control

Suppose $x(t) \in X \subset \mathbb{R}^n$ represents the state variables of a system and $u(t) \in U \subset \mathbb{R}^m$ represents the control variables at time t, with $t_0 \le t \le t_f$. An optimal control problem consists of finding a piecewise continuous control $u(t)$ and the associated state $x(t)$ that optimizes a cost function $J[u(t), x(t)]$. The majority of mathematical models that use the optimal control theory rely on Pontryagin's Maximum Principle, a first-order condition for finding the optimal solution.

Theorem 1. *(Pontryagin's Maximum Principle [48]) If $u^*(t)$ and $x^*(t)$ are optimal for the problem*

$$\max_u J[u(t), x(t)], \qquad (1)$$

where

$$J\left[u(t), x\left(t\right)\right] = \max_{u} \int_{t_0}^{t_f} f\left(t, x\left(t\right), u\left(t\right)\right) dt,$$

subject to

$$\begin{cases} \dfrac{dx}{dt} = g\left(t, x\left(t\right), u\left(t\right)\right), \\ x\left(t_0\right) = x_0, \end{cases}$$

then there exists a piecewise differentiable adjoint variable $\lambda\left(t\right)$ such that

$$H(t, x^*(t), u(t), \lambda(t)) \leq H(t, x^*(t), u^*(t), \lambda(t)))$$

for all controls u at each time t, where the Hamiltonian H is given by

$$\begin{aligned} &H(t, x(t), u(t), \lambda(t)) \\ &= f\left(t, x\left(t\right), u\left(t\right)\right) + \lambda g\left(t, x\left(t\right), u\left(t\right)\right) \quad (2) \end{aligned}$$

and

$$\begin{cases} \lambda'\left(t\right) = -\dfrac{\partial H\left(t, x^*\left(t\right), u^*\left(t\right), \lambda\left(t\right)\right)}{\partial x}, \\ \lambda\left(t_f\right) = 0. \end{cases}$$

While Pontryagin's Maximum Principle gives the necessary conditions for the existence of an optimal solution, the following theorem provides sufficient conditions.

Theorem 2. *(Arrow Sufficiency Theorem [49]) For the optimal control problem (1), the conditions of the maximum principle are sufficient for the global minimization of $J\left[u(t), x\left(t\right)\right]$, if the minimized Hamiltonian function H, defined in (2), is convex in the variable x for all t in the time interval $[t_0, t_f]$ for a given λ.*

One of the major side effects of vaccination/treatment is the creation of drug resistant virus/bacteria which eventually leads to drug failure (due to ineffectiveness of the vaccine/treatment). Optimal control has been used to curb the creation of drug resistant virus/bacteria or drug failure (at the same time reducing the cost of treatment or vaccination) by imposing a condition that monitors the global effect of the vaccination/treatment program. Hence if $x(t)$ represents the group of individuals to be vaccinated/treated

and $u(t) \in U$ represents the control on vaccination/treatment, where the control set U is given by

$$U = \{u(t) : v_0 \leq u(t) \leq v_1, \text{ Lebesgue measurable}\},$$

then, the following objective functions are to be minimized simultaneously:

$$\begin{aligned} I_1\left(u\right) &= \int_{t_0}^{t_f} x\left(t\right) dt \text{ and} \\ I_2\left(u\right) &= \int_{t_0}^{t_f} u^m\left(t\right) dt, \text{ for } m > 0, \end{aligned}$$

and the optimal solution can be represented as

$$\min_{u} \{I_1\left(u\right), I_2\left(u\right)\}.$$

In general, there does not exist a feasible solution that minimizes both objective functions simultaneously. Hence, the Pareto optimality concept is used to simultaneously find optimal control u^* that minimizes both objective functions.

III. DERIVATION AND PRELIMINARIES OF COVID-19 MODEL

This section develops a mathematical model of COVID-19 transmission with the subsequent suppositions: The underlying human population is split up into six mutually exclusive compartments, namely, susceptible (S), exposed (infected but not yet infectious) (E), home quarantined population (population were exposed to the virus but viewing light symptoms of coronavirus disease and stay at home isolation) (H), government quarantined population (population was infective in symptomatic phase, i.e., showing symptoms of coronavirus disease and stay at Government observation places for isolation) (G), infected (I), and recovered class (R) (infectious people who have cleared or recovered from coronavirus infection). Therefore, the total human population $N(t) = S(t) + E(t) + H(t) + G(t) + I(t) + R(t)$.

This model involves certain assumptions which consist of the following:

(i) The susceptible population (S) comprises individuals who have not yet been infected by Covid-19, but may be infected through

contact with both types of home quarantined (H) and government quarantined (G) people.

(ii) The exposed population (E) comprises individuals infected with Covid-19 infection but not infectious.

(iii) The infective population in home quarantined phase (H) comprises individuals who have Covid-19 infection with light symptoms (but capable of infecting) and quarantined at home for isolation.

(iv) The infective population in the symptomatic phase (G) comprises individuals who have developed Covid-19 infection with complications and various symptoms but their test report yet not come positive and are quarantined by the Government facility for isolation.

(v) The infected population (I), whose COVID 19 test is positive clinically and stayed at hospital for treatment (incapable of infecting others). The infected individuals coming from home and Government quarantined compartments if their test report comes positive.

(vi) The recovered class (R) consists of those who become healed from the disease by treatment or quarantined program.

(vii) The susceptible individuals become infected by adequate contact with infective individuals in the asymptomatic phase (home quarantined) and symptomatic phase (Government quarantined), and enter into the exposed class. The susceptible population is also decreased due to natural death.

(viii) The exposed population is entered into the home quarantined, government quarantined, and infected population, respectively. The said population is also diminished due to natural death.

(ix) One part of home quarantined individuals enters into the infected population, and the other becomes recovered. This population is also decreased by natural death.

(x) One part of the government quarantined individuals enters into the infected population, and the other becomes recovered. This individual is also decreased by natural death.

(xi) One part of the infected population enters into the recovered class. Other individuals are decreased due to infection and natural death.

(xii) Home quarantined (asymptomatic), government quarantined (symptomatic), and the infected population recover from the coronavirus disease and enters into the recovered class. The recovered population diminishes by natural death.

The parameters of the Covid-19 model are presented as follows:

Λ : The recruitment rate of susceptible from embedding population.

α_1 : The coefficient of transmission rate from home quarantined to susceptible individuals, and the expression gives the transmission rate: $\alpha_1 H(t)S(t)$.

α_2 : The coefficient of transmission rate from Government quarantined population to susceptible individuals, and the transmission rate is: $\alpha_2 G(t)S(t)$.

β_1 : The fraction of exposed individuals that will start to show light symptoms of Covid-19 (but remains capable of infecting others) and move to the class H.

β_2 : The rate at which the exposed individuals become infected by Covid 19 infection and move to the class I.

β_3 : The fraction of the exposed individuals that will start to show symptoms of infection and move to the class G.

γ_2 : The rate of home quarantined individuals eventually show disease symptoms and move to class I.

γ_1 : The recovery rate of the home quarantined population H.

σ_2 : The rate at which government quarantined individuals eventually show disease symptoms and move to class I.

σ_1 : The recovery rate of the Government quarantined population G.

d_2 : The disease-related death rate of infective population in the infected phase I

ϵ : The recovery rate of the infected population I.

d_1 : The natural death rate of all human epidemiological classes.

In our proposed Covid-19 model, $S(t)$, $E(t)$, $H(t)$, $G(t)$, $I(t)$, and $R(t)$ denote the numbers of susceptible, exposed, home quarantined, government quarantined, infected, and recovered, respectively. Through the contact between susceptible and home quarantined populations, a part of the susceptible population, i.e., $\alpha_1 H(t)S(t)$, becomes infected and enters into exposed class. Similarly, through the contact between susceptible and government quarantined populations, a part of the susceptible people, i.e., $\alpha_2 G(t)S(t)$, becomes infected and enters into the exposed category. The fraction of the home quarantined population γ_2 will start to show symptoms of and move to the class I. Another portion of the home quarantined population γ_1 is recovered from infection due to treatment or quarantined process and move to the recovered class R. Similarly, a fraction of the government quarantined community σ_2 will start to show symptoms of Covid 19 and move to the class I. Other portion of the home quarantined population σ_1 is recovered from infection due to treatment or quarantined process and move to the recovered class R. A fraction of infected individuals ϵ is recovered from infection through treatment in Hospital and move to recovered class R. Another fraction d_2 of the infected individuals is diminished due to the disease-related death rate of the infective population. From every class, a part of the inhabitants is reduced at the natural death rate d_1.

We diagrammatically represent the flow of individuals from one class to another in Fig. 1.

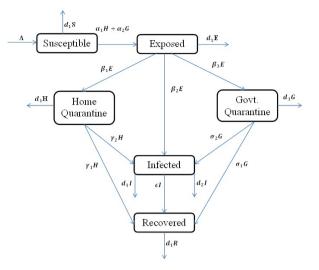Therefore, our proposed mathematical model of the Covid-19 infection is presented through the

Fig. 1. Pictorial representation of proposed Covid 19 model for Indian scenario

following set of non-linear differential equation

$$\frac{dS}{dt} = \Lambda - (\alpha_1 H + \alpha_2 G) S - d_1 S, \qquad (3)$$

$$\frac{dE}{dt} = (\alpha_1 H + \alpha_2 G) S - (\beta_1 + \beta_2 + \beta_3 + d_1) E,$$

$$\frac{dH}{dt} = \beta_1 E - \gamma_1 H - \gamma_2 H - d_1 H,$$

$$\frac{dG}{dt} = \beta_3 E - \sigma_1 G - \sigma_2 G - d_1 G,$$

$$\frac{dI}{dt} = \beta_2 E + \gamma_2 H + \sigma_2 G - d_1 I - d_2 I - \epsilon I,$$

$$\frac{dR}{dt} = \epsilon I - d_1 R + \gamma_1 H + \sigma_1 G;$$

with initial conditions:

$$S(0) > 0, E(0) \geq 0, H(0) \geq 0,$$
$$G(0) \geq 0, I(0) \geq 0, R(0) \geq 0. \qquad (4)$$

The SEHGIR model formulation (3) can be

rewritten as:

$$\frac{dS}{dt} = \Lambda - (\alpha_1 H + \alpha_2 G)\, S - d_1 S, \quad (5)$$

$$\frac{dE}{dt} = (\alpha_1 H + \alpha_2 G)\, S - AE,$$

$$\frac{dH}{dt} = \beta_1 E - BH,$$

$$\frac{dG}{dt} = \beta_3 E - CG,$$

$$\frac{dI}{dt} = \beta_2 E + \gamma_2 H + \sigma_2 G - DI,$$

$$\frac{dR}{dt} = \gamma_1 H + \sigma_1 G + \epsilon I - d_1 R;$$

where

$$A = \beta_1 + \beta_2 + \beta_3 + d_1,$$
$$B = \gamma_1 + \gamma_2 + d_1,$$
$$C = \sigma_1 + \sigma_2 + d_1,$$
$$D = d_1 + d_2 + \epsilon,$$

with initial conditions (4).

IV. FUNDAMENTAL PROPERTIES

A. Positivity of the solutions

Theorem 3. *Each solution of the proposed system (5) under conditions (4) satisfy $S(t) > 0$, $E(t) \geq 0$, $H(t) \geq 0$, $G(t) \geq 0$, $I(t) \geq 0$, $R(t) \geq 0$ for all values of $t \geq 0$.*

Proof: The first equation of the system (5), can be written

$$\begin{aligned}\frac{dS}{dt} &= \Lambda - (\alpha_1 H + \alpha_2 G)\, S - d_1 S \\ &= \Lambda - \psi S;\end{aligned}$$

where $\psi = (\alpha_1 H + \alpha_2 G) - d_1$. Thereafter by integration, we obtain the following expression

$$\begin{aligned}S(t) = &S(0) \exp\left(-\int_0^t \psi(s)ds\right) \\ &+ \Lambda \exp\left(-\int_0^t \psi(s)ds\right)\int_0^t e^{\int_0^t \psi(v)dv}ds > 0.\end{aligned}$$

Hence $S(t)$ is non-negative for all t. From the next equation of (5), we get,

$$\frac{dE}{dt} \geq -AE.$$

This equation provides

$$E(t) \geq E(0)\exp(-At) \geq 0.$$

Also, from the remaining equations and with the help of initial conditions, we obtain

$$H(t) \geq H(0)\exp(-Bt) \geq 0,$$
$$G(t) \geq G(0)\exp(-Ct) \geq 0,$$
$$I(t) \geq I(0)\exp(-Dt) \geq 0,$$

as well as

$$R(t) \geq R(0)\exp(-d_1 t) \geq 0.$$

So, it is observed that $S(t) > 0$, $E(t) \geq 0$, $H(t) \geq 0$, $G(t) \geq 0$, $I(t) \geq 0$, $R(t) \geq 0$ for all values of $t \geq 0$. Hence the theorem. ∎

B. Invariant region

Theorem 4. *The feasible region Γ defined by*

$$\Gamma = \left\{ (S, E, H, G, I, R) \in \mathbb{R}_+^6 : 0 < N \leq \frac{\Lambda}{\eta} \right\},$$

where $\eta = \min\{d_1, d_1 + d_2\}$ is positively invariant for the system (3).

Proof: Let

$$((S(0), E(0), H(0), G(0), I(0), R(0)) \in \Gamma.$$

Adding the equations of the system (3) we obtain

$$\frac{dN}{dt} = \Lambda - d_1 S - d_1 E - d_1 H - d_1 H - d_1 G - (d_1 + d_2)I - d_1 R.$$

Therefore,

$$\begin{aligned}\frac{dN}{dt} + \eta N = &\Lambda - (d_1 - \eta)S - (d_1 - \eta)E - d_1 H \\ &- (d_1 - \eta)H - (d_1 - \eta)G - (d_1 + d_2 - \eta)I \quad (6) \\ &- (d_1 - \eta)R \leq \Lambda,\end{aligned}$$

where $\eta = \min\{d_1, d_1 + d_2\}$. The solution N(t) of the differential equation (6) has the following property,

$$0 < N(t) \leq N(0)\exp(-\eta t) + \frac{\Lambda}{\eta}(1 - \exp(-\eta t)),$$

where $N(0)$ represents the sum of the initial values of the variables. As $t \to \infty$, we have $0 < N(t) \leq \frac{\Lambda}{\eta}$. Also, if $N(0) \leq \frac{\Lambda}{\eta}$ then $N(t) \leq \frac{\Lambda}{\eta}$

for all t. This means $\frac{\Lambda}{\eta}$ is the upper bound of N. On the other hand, if $N(0) > \frac{\Lambda}{\eta}$ implies $N(t)$ will decrease to $\frac{\Lambda}{\eta}$. This means that if $N(0) > \frac{\Lambda}{\eta}$, the solution $(S(t), E(t), H(t), G(t), I(t), R(t))$ enters Γ or approaches it asymptotically. Hence it is positively invariant under the flow induced by the systems (3) and (4). ∎

Thus in Γ the mathematical model (3) with initial conditions (4) is well-posed epidemiologically. Hence it is sufficient to study the dynamics of the model in Γ.

V. EXISTENCE OF EQUILIBRIUM AND STABILITY ANALYSIS

In this section, we will study the existence and stability behavior of the system (3) at various equilibrium points. The equilibrium points of the system (2.1) are:

(i) Disease-free equilibrium (DFE):

$$E_0\left(\frac{\Lambda}{d_1}, 0, 0, 0, 0, 0\right),$$

(ii) Endemic equilibrium:

$$E_1(S^*, E^*, H^*, G^*, I^*, R^*).$$

A. *The basic reproduction number*

The basic reproduction number (BRN) ([50]-[53]) of the system (3) will be obtained by the next-generation matrix method [54].

Let $z = (E(t), H(t), G(t), I(t), S(t), R(t))^T$, the proposed Covid-19 system (3) can be written in the following form:

$$\frac{dz}{dt} = F(z) - \upsilon(z);$$

where

$$F(z) = \begin{bmatrix} (\alpha_1 H + \alpha_2 G) S \\ 0 \\ 0 \\ 0 \\ 0 \\ 0 \end{bmatrix},$$

$$\upsilon(z) = \begin{bmatrix} AE \\ -\beta_1 E + BH \\ -\beta_3 E + CG \\ -(\beta_2 E + \gamma_2 H + \sigma_2 G) + DI \\ -(\gamma_1 H + \sigma_1 G + \epsilon I) + d_1 R \\ -\Lambda + (\alpha_1 H + \alpha_2 G) S + d_1 S \end{bmatrix}.$$

The Jacobian matrices of $F(z)$ and $\upsilon(z)$ at the DFE E_0 are as follows, respectively:

$$DF(E_0) = \begin{bmatrix} F_{4\times4} & 0 & 0 \\ 0 & 0 & 0 \\ 0 & 0 & 0 \end{bmatrix},$$

$$D\upsilon(E_0) = \begin{bmatrix} V_{4\times4} & 0 & 0 \\ 0 & 0 & 0 \\ 0 & 0 & 0 \end{bmatrix},$$

where

$$F = \begin{bmatrix} 0 & \frac{\Lambda\alpha_1}{d_1} & \frac{\Lambda\alpha_2}{d_1} & 0 \\ 0 & 0 & 0 & 0 \\ 0 & 0 & 0 & 0 \\ 0 & 0 & 0 & 0 \end{bmatrix},$$

$$V = \begin{bmatrix} A & 0 & 0 & 0 \\ -\beta_1 & B & 0 & 0 \\ -\beta_3 & 0 & C & 0 \\ -\beta_2 & -\gamma_2 & -\sigma_2 & D \end{bmatrix}.$$

Following [54], $R_0 = \rho\left(FV^{-1}\right)$ where ρ is the spectral radius of the next-generation matrix (FV^{-1}). Thus, from the model (3), we have the following expression for BRN R_0 :

$$R_0 = \frac{\Lambda}{d_1}\frac{1}{ABC}[\alpha_1\beta_1 C + \alpha_2\beta_3 B].$$

Notice that $\frac{\Lambda}{d_1}$ is the number of susceptibles at the DFE.

B. *Existence of endemic equilibrium $E_1(S^*, E^*, H^*, G^*, I^*, R^*)$*

In this section, we will analyze the existence of a non-trivial endemic equilibrium $E_1(S^*, E^*, H^*, G^*, I^*, R^*)$ of the system (3). To find the endemic equilibrium of the system (3), we consider the following:

$$S(t) > 0, E(t) > 0, H(t) > 0,$$
$$G(t) > 0, I(t) > 0, R(t) > 0$$

and

$$\frac{dS}{dt}=0,\ \frac{dE}{dt}=0,\ \frac{dH}{dt}=0,\ \frac{dG}{dt}=0,\ \frac{dR}{dt}=0. \quad (7)$$

From the third, fourth, fifth, and sixth equation of (7) we obtain

$$H^* = \frac{\beta_1 E^*}{B},\ G^* = \frac{\beta_3 E^*}{C},$$
$$I^* = \frac{E^*}{D}[\beta_2 + \frac{\gamma_2 \beta_1}{B} + \frac{\beta_3 \sigma_2}{C}],$$
$$R^* = \frac{E^*}{d_1}\left[\frac{\epsilon}{D}\{\beta_2 + \frac{\gamma_2 \beta_1}{B} + \frac{\beta_3 \sigma_2}{C}\} + \frac{\gamma_1 \beta_1}{B} + \frac{\beta_3 \sigma_1}{C}\right].$$

Now from $\frac{dE}{dt} = 0$ and using the values of H^* and G^*, we get,

$$S^* = \frac{\Lambda}{d_1 R_0} > 0.$$

Again, putting the value of S^* in the first equation of (7) we gain,

$$E^* = \frac{\Lambda}{A}\left[1 - \frac{1}{R_0}\right].$$

Hence, E^* has a unique positive solution iff $R_0 > 1$.

Summarizing the above discussions, we arrive at the following result.

Theorem 5. *The system (3) has a DFE $E_0(\frac{\Lambda}{d_1}, 0, 0, 0, 0, 0)$, which exists for all parameter values. If $R_0 > 1$ the system (3) also admits a unique endemic equilibrium $E_1(S^*, E^*, H^*, G^*, I^*, R^*)$.*

C. Asymptotic behavior

For the stability of DFE $E_0(\frac{\Lambda}{d_1}, 0, 0, 0, 0, 0)$ we consider the theorems given below

Theorem 6. *The DFE E_0 of the system (3) is locally asymptotically stable if $R_0 < 1$.*

Proof: See Appendix A. ∎

Theorem 7. *The diseases free equilibrium (DFE) $E_0(\frac{\Lambda}{d_1}, 0, 0, 0, 0, 0)$ is globally asymptotically stable (GAS) in $\mathbb{R}_+^6$ for the system (3) if $R_0 < 1$ and becomes unstable if $R_0 > 1$.*

Proof: We rewrite the system (3) as

$$\frac{dX}{dt} = F(X, V),$$
$$\frac{dV}{dt} = G(X, V),\ G(X, 0) = 0,$$

where $X = (S, R) \in \mathbb{R}^2$ (the number of uninfected individuals compartments), $V = (E, H, G, I) \in \mathbb{R}^4$ (the number of infected individuals compartments), and $E_0(\frac{\Lambda}{d_1}, 0, 0, 0, 0, 0)$ is the DFE of the system (3). The global stability of the DFE is guaranteed if the following two conditions are satisfied:

(i) For $\frac{dX}{dt} = F(X, 0)$, X^* is globally asymptotically stable in $\mathbb{R}^2$.

(ii) $G(X, V) = BV - \widehat{G}(X, V)$, $\widehat{G}(X, V) \geq 0$ for $(X, V) \in \Omega$,

where $B = D_V G(X^*, 0)$ is a Metzler matrix, and Ω is the positively invariant set to the model (3). Following Castillo-Chavez et al. [55], we check for aforementioned conditions. For system (3),

$$F(X, 0) = \begin{bmatrix} \Lambda - d_1 S \\ 0 \end{bmatrix},$$

$$B = \begin{bmatrix} -A & \frac{\Lambda \alpha_1}{d_1} & \frac{\Lambda \alpha_2}{d_1} & 0 \\ \beta_1 & -B & 0 & 0 \\ \beta_3 & 0 & -C & 0 \\ \beta_2 & \gamma_2 & \sigma_2 & -D \end{bmatrix}$$

and

$$\widehat{G}(X, V) = \begin{bmatrix} (\frac{\Lambda}{d_1} - S)(\alpha_1 H + \alpha_2 G) \\ 0 \\ 0 \\ 0 \end{bmatrix}.$$

Clearly, $\widehat{G}(X, V) \geq 0$ (using Theorem 2), whenever the state variables are inside Ω (the positively invariant set of the model (3)). Again, it is clear that $X^* = (\frac{\Lambda}{d_1}, 0)^T$ is a globally asymptotically stable equilibrium of the system $\frac{dX}{dt} = F(X, 0)$. Hence, the theorem follows. ∎

Theorem 8. *The endemic equilibrium point $E_1(S^*, E^*, H^*, G^*, I^*, R^*)$ of the system (3) is locally asymptotically stable if $R_0 > 1$, $B_1 B_2 - B_3 > 0$ and $B_1 B_2 B_3 - B_1^2 B_4 - B_3^2 > 0$*

Proof: See Appendix B. ∎

VI. PROPOSED COVID-19 MODEL WITH CONTROL

In this section, the primary focus is to set up an optimal control problem of the epidemic model (3). In the present situation of the Covid-19 outbreak, it is highly essential to construct an optimal control problem so that the total amount of drug is minimized. Here we take one control variable $u(t)$ on the recovery rate of the infectious individuals in the infected phase with treatment in the hospital. Therefore, our epidemic model with one control and the same initial conditions (4) becomes:

$$
\begin{aligned}
\frac{dS}{dt} &= \Lambda - (\alpha_1 H(t) + \alpha_2 G(t)) \, S(t) - d_1 S(t), \\
\frac{dE}{dt} &= (\alpha_1 H + \alpha_2 G) \, S - (\beta_1 + \beta_2 + \beta_3 + d_1) \, E, \\
\frac{dH}{dt} &= \beta_1 E - \gamma_1 H - \gamma_2 H - d_1 H, \\
\frac{dG}{dt} &= \beta_3 E - \sigma_1 G - \sigma_2 G - d_1 G, \\
\frac{dI}{dt} &= \beta_2 E(t) + \gamma_2 H(t) + \sigma_2 G(t) \\
&\quad - (d_1 + d_2) I(t) - u(t) I(t), \\
\frac{dR}{dt} &= u(t) I(t) + \gamma_1 H(t) + \sigma_1 G(t) - d_1 R(t).
\end{aligned} \tag{8}
$$

The control function $u(t)$, $0 \le u(t) \le 1$ represents the fraction of the infected individuals who are identified and will be treated. When $u(t)$ is close to 1 then the treatment failure is low, but the implementation cost is high. For the model (8), the single-objective cost functional to be minimized is given by the objective functional ([56]-[59])

$$
J(u(t)) = \int_0^{t_f} [G_1 I + \frac{1}{2} G_2 u^2] dt; \tag{9}
$$

with $G_1 > 0$ and $G_2 > 0$, where we want to minimize the infectious group I while also keeping the cost of treatment $u(t)$ low. The term $G_1 I$ represents the cost of infection, while the term $\frac{1}{2} G_2 u^2$ represents the cost of treatment. The goal is to find an optimal control, u^*, such that

$$
J(u^*) = \min\{J(u) : u \in U\}, \tag{10}
$$

where

$$
\begin{aligned}
U = \{ u : u \text{ is Lebesgue measurable,} \\
0 \le u \le 1,\ t \in [0,\ t_f] \}
\end{aligned} \tag{11}
$$

Applying the Pontryagins Maximum Principle, we have the following result $\left(\overline{S}^*, \overline{E}^*, \overline{H}^*, \overline{G}^*, \overline{I}^*, \overline{R}^*\right)$ of the system (8), that minimizes $J(u)$ over U.

Theorem 9. *There exists an optimal control u^* and corresponding solutions $\left(\overline{S}^*, \overline{E}^*, \overline{H}^*, \overline{G}^*, \overline{I}^*, \overline{R}^*\right)$ of the system (8), that minimizes $J(u)$ over U. Furthermore, there exist adjoint functions $\lambda_i(t)$, $i = 1, 2, 3, 4, 5, 6$, such that*

$$
\begin{aligned}
\frac{d\lambda_1}{dt} &= (\lambda_1 - \lambda_2)(\alpha_1 H + \alpha_2 G) + \lambda_1 d_1, \\
\frac{d\lambda_2}{dt} &= (\lambda_2 - \lambda_3)\beta_1 + (\lambda_2 - \lambda_5)\beta_2 + (\lambda_2 - \lambda_4)\beta_3 \\
&\quad + \lambda_2 d_1, \\
\frac{d\lambda_3}{dt} &= (\lambda_1 - \lambda_2)\alpha_1 S + (\lambda_3 - \lambda_6)\gamma_1 + (\lambda_3 - \lambda_5)\gamma_2 \\
&\quad + \lambda_3 d_1, \\
\frac{d\lambda_4}{dt} &= (\lambda_1 - \lambda_2)\alpha_2 S + (\lambda_4 - \lambda_6)\sigma_1 + (\lambda_4 - \lambda_5)\sigma_2 \\
&\quad + \lambda_4 d_1, \\
\frac{d\lambda_5}{dt} &= (\lambda_5 - \lambda_6)u + (d_1 + d_2)\lambda_5 - G_1, \\
\frac{d\lambda_6}{dt} &= d_1 \lambda_6;
\end{aligned}
$$

with transversality conditions

$$
\lambda_i(t_f) = 0,\ i = 1, 2, 3, 4, 5, 6,
$$

and the control u^* satisfies the optimality condition

$$
u^* = \min\{\max\{0, \frac{(\lambda_5 - \lambda_6)\overline{I}^*}{G_2}\}, 1\}.
$$

Proof: The Hamiltonian is defined as follows:

$$
\begin{aligned}
\hat{H} &= G_1 I + \frac{1}{2} G_2 u^2 + \lambda_1 [\Lambda - (\alpha_1 H + \alpha_2 G) \, S - d_1 S] \\
&\quad + \lambda_2 [(\alpha_1 H + \alpha_2 G) \, S - AE] \\
&\quad + \lambda_3 [\beta_1 E - BH] + \lambda_4 [\beta_3 E - CG] \\
&\quad + \lambda_5 [\beta_2 E + \gamma_2 H + \sigma_2 G - (d_1 + d_2) I - uI] \\
&\quad + \lambda_6 [uI + \gamma_1 H + \sigma_1 G - d_1 R],
\end{aligned} \tag{12}
$$

where λ_i $(i = 1, 2, 3, 4, 5, 6)$ are the adjoint functions to be determined.

The form of the adjoint equations and transversality conditions are expected results from Pontryagin's Maximum Principle [60]. The adjoint system can be obtained as follows:

$$
\begin{aligned}
\frac{d\lambda_1}{dt} &= -\frac{\partial \hat{H}}{\partial S} = (\lambda_1 - \lambda_2)(\alpha_1 H + \alpha_2 G) + \lambda_1 d_1, \\
\frac{d\lambda_2}{dt} &= -\frac{\partial \hat{H}}{\partial E} = (\lambda_2 - \lambda_3)\beta_1 + (\lambda_2 - \lambda_5)\beta_2 \\
&\qquad\qquad + (\lambda_2 - \lambda_4)\beta_3 + \lambda_2 d_1, \\
\frac{d\lambda_3}{dt} &= -\frac{\partial \hat{H}}{\partial H} = (\lambda_1 - \lambda_2)\alpha_1 S + (\lambda_3 - \lambda_6)\gamma_1 \\
&\qquad\qquad + (\lambda_3 - \lambda_5)\gamma_2 + \lambda_3 d_1, \\
\frac{d\lambda_4}{dt} &= -\frac{\partial \hat{H}}{\partial G} = (\lambda_1 - \lambda_2)\alpha_2 S + (\lambda_4 - \lambda_6)\sigma_1 \\
&\qquad\qquad + (\lambda_4 - \lambda_5)\sigma_2 + \lambda_4 d_1, \\
\frac{d\lambda_5}{dt} &= -\frac{\partial \hat{H}}{\partial I} = (\lambda_5 - \lambda_6)u + (d_1 + d_2)\lambda_5 - G_1, \\
\frac{d\lambda_6}{dt} &= -\frac{\partial \hat{H}}{\partial R} = d_1 \lambda_6.
\end{aligned}
\tag{13}
$$

The transversality conditions (or boundary conditions) are

$$
\lambda_i(t_f) = 0, \; i = 1, 2, 3, 4, 5, 6. \tag{14}
$$

By the optimality condition, at $u = u^*(t)$ we have

$$
\begin{aligned}
\frac{\partial \hat{H}}{\partial u} &= G_2 u^* - (\lambda_5 - \lambda_6)\overline{I}^* = 0 \\
&\Rightarrow u^*(t) = \frac{(\lambda_5 - \lambda_6)\overline{I}^*}{G_2}.
\end{aligned}
\tag{15}
$$

By using the bounds for the control $u(t)$, we get

$$
u^* = \begin{cases}
\frac{(\lambda_5 - \lambda_6)\overline{I}^*}{G_2}, & \text{if } 0 \le \frac{(\lambda_5 - \lambda_6)\overline{I}^*}{G_2} \le 1. \\
0, & \text{if } \frac{(\lambda_5 - \lambda_6)\overline{I}^*}{G_2} \le 0. \\
1, & \text{if } \frac{(\lambda_5 - \lambda_6)\overline{I}^*}{G_2} \ge 1.
\end{cases}
$$

In compact notation:

$$
u^* = \min\left\{ \max\left\{ 0, \frac{(\lambda_5 - \lambda_6)\overline{I}^*}{G_2} \right\}, 1 \right\}. \tag{16}
$$

Using (16), we obtain the following optimality system:

$$
\frac{dS}{dt} = \Lambda - (\alpha_1 H + \alpha_2 G)S - d_1 S, \tag{17}
$$

$$
\frac{dE}{dt} = (\alpha_1 H + \alpha_2 G)S - AE,
$$

$$
\frac{dH}{dt} = \beta_1 E - BH,
$$

$$
\frac{dG}{dt} = \beta_3 E - CG,
$$

$$
\frac{dI}{dt} = \beta_2 E + \gamma_2 H + \sigma_2 G - (d_1 + d_2)I
$$
$$
\qquad - \min\left\{ \max\left\{ 0, \frac{(\lambda_5 - \lambda_6)\overline{I}^*}{G_2} \right\}, 1 \right\} I,
$$

$$
\frac{dR}{dt} = \min\left\{ \max\left\{ 0, \frac{(\lambda_5 - \lambda_6)\overline{I}^*}{G_2} \right\}, 1 \right\} I
$$
$$
\qquad + \gamma_1 H + \sigma_1 G - d_1 R,
$$

$$
\frac{d\lambda_1}{dt} = (\lambda_1 - \lambda_2)(\alpha_1 H + \alpha_2 G) + \lambda_1 d_1,
$$

$$
\frac{d\lambda_2}{dt} = (\lambda_2 - \lambda_3)\beta_1 + (\lambda_2 - \lambda_5)\beta_2
$$
$$
\qquad + (\lambda_2 - \lambda_4)\beta_3 + \lambda_2 d_1,
$$

$$
\frac{d\lambda_3}{dt} = (\lambda_1 - \lambda_2)\alpha_1 S + (\lambda_3 - \lambda_6)\gamma_1
$$
$$
\qquad + (\lambda_3 - \lambda_5)\gamma_2 + \lambda_3 d_1,
$$

$$
\frac{d\lambda_4}{dt} = (\lambda_1 - \lambda_2)\alpha_2 S + (\lambda_4 - \lambda_6)\sigma_1
$$
$$
\qquad + (\lambda_4 - \lambda_5)\sigma_2 + \lambda_4 d_1,
$$

$$
\frac{d\lambda_5}{dt} = (\lambda_5 - \lambda_6)\min\left\{ \max\{ 0, \frac{(\lambda_5 - \lambda_6)\overline{I}^*}{G_2} \}, 1 \right\}
$$
$$
\qquad + (d_1 + d_2)\lambda_5 - G_1,
$$

$$
\frac{d\lambda_6}{dt} = d_1 \lambda_6;
$$

subject to the following conditions:

$$
S(0) > 0, \; E(0) \ge 0, \; H(0) \ge 0,
$$
$$
G(0) \ge 0, \; I(0) \ge 0, \; R(0) \ge 0
$$

and

$$
\lambda_1(t_f) = 0, \; \lambda_2(t_f) = 0, \; \lambda_3(t_f) = 0,
$$
$$
\lambda_4(t_f) = 0, \; \lambda_5(t_f) = 0, \; \lambda_6(t_f) = 0.
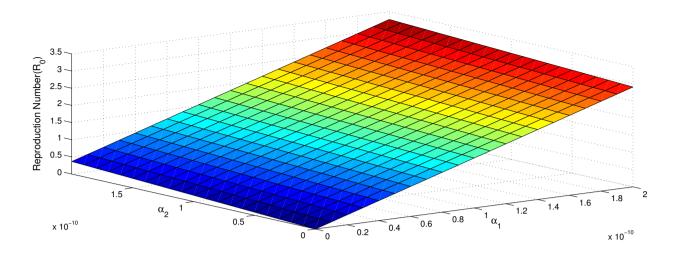$$

This completes the proof. ∎

Fig. 2. Sensitivity of R_0 to α_1 and α_2, rest of the parameters are based on Table 1

VII. NUMERICAL SIMULATIONS

The current section presents some computer simulations to assess the proposed model's applicability for the Covid-19 scenario. The simulation is carried out based on available data of pandemic infection in India. Also, these numerical simulation is very much crucial from a practical viewpoint.

Estimating the parameters of the model for India, we have studied the proposed Covid-19 system. The main objective is to study the effects of two quarantined population parameters α_1 and α_2, to show the impact of these parameters on the pandemic curve through the graphical presentation. By changing the values of the mentioned parameters, we observe the infected population's behavior for 60 days from 2nd April for their particular base values. Table 1 and Table 2 give the values of the model parameters and initial population density, respectively.

Based on Table 1, the BRN is $R_0 = 3.0909$, which is much greater than one. Hence the infection spread so quickly in India. Therefore, it needs to take the right policy to reduce the value of R_0 much less to 1. For the proposed model, a graphical presentation of R_0 to α_1 and α_2 is given in Figure 2.
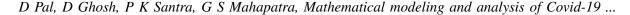
TABLE I
MODEL PARAMETERS FOR COVID-19 SYSTEM

Parameters	Values (**Unit**)	Data Source
Λ	50000 **day**$^{-1}$	[61]
α_1	2×10^{-10} **day**$^{-1}$	Estimated
α_2	1×10^{-10} **day**$^{-1}$	Estimated
β_1	0.4 **day**$^{-1}$	Assumed
β_2	1×10^{-6} **day**$^{-1}$	Assumed
β_3	0.05 **day**$^{-1}$	Assumed
γ_1	0.15 **day**$^{-1}$	Estimated
γ_2	0.0028 **day**$^{-1}$	Estimated
σ_1	0.15 **day**$^{-1}$	Estimated
σ_2	0.002 **day**$^{-1}$	Estimated
ϵ	0.06 **day**$^{-1}$	Estimated
d_1	2×10^{-5} **day**$^{-1}$	[61]
d_2	0.001 **day**$^{-1}$	Estimated

TABLE II
PRELIMINARY POPULATION DENSITY FOR COVID-19 MODEL

$S(0)$	$E(0)$	$H(0)$	$G(0)$	$I(0)$	$R(0)$
12×10^8	2×10^5	2×10^5	5×10^4	1649	5×10^4

In Figure 3, the 'red' curve presents an infected individual for this proposed model, and the bar diagram is the actual infected individual as per our available data. Figure 3 depicts that the actual infected individual almost coincides with our
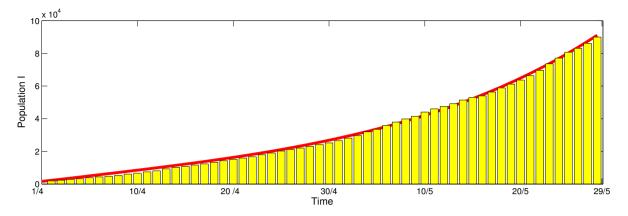
Fig. 3. Time series of infected population with parameter values and initial conditions from Table 1 and 2 during $1/4/2020$ to $29/5/2020$.
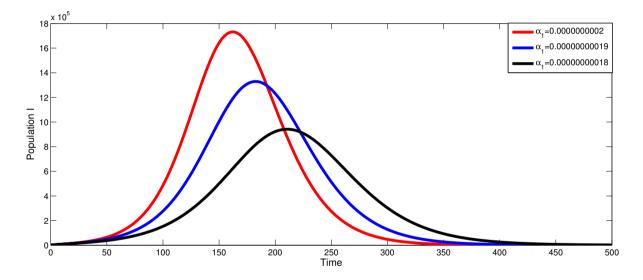

Fig. 4. Time series of the infected population with $\alpha_2 = 1 \times 10^{-10}$ for different values of α_1 and other input values taken from Table 1 and 2.

proposed model curve from 1st April to 29th May 2020. Therefore, the proposed Covid-19 model is best fitted to the current situation of India.

For fixed α_2 if we gradually decrease α_1, the infected individuals is also reduces steadily, which is presented via Figure 4.

Therefore, practically if we strictly follow the home quarantined restriction, then naturally α_1 decrease, and also the pick of the infected individual reduces. It is also observed from Figure 4 that for $\alpha_1 = 2 \times 10^{-10}$, the pick of the disease reached

almost after 160 days from 1st April 2020, and the height number of infected cases around 1700000. For $\alpha_1 = 1.9 \times 10^{-10}$ and $\alpha_1 = 1.8 \times 10^{-10}$ the pick of infection reached almost after 175 and 220 days, respectively from 1st April 2020, and the corresponding height number of infected cases may be around 1200000 and 800000, respectively.

Again if we fixed α_1 at 2×10^{-10} and the values of α_2 gradually increase, then the infected number of individuals is also gradually increasing, which
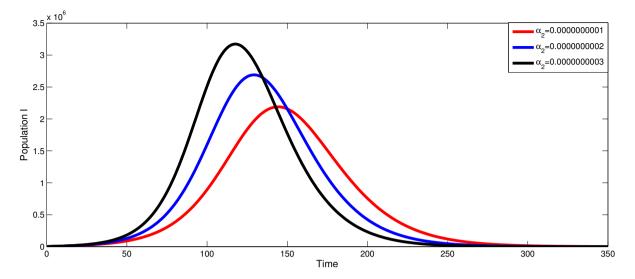
Fig. 5. Time series of infected population with parameter values and initial conditions from Table 1 and 2 during $1/4/2020$ to $29/5/2020$.
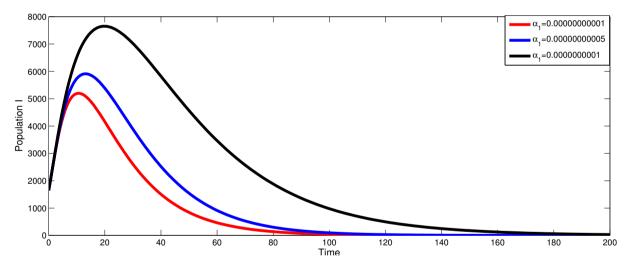

Fig. 6. Time series of infected population with $\alpha_1 = \alpha_2$ using data from Table 1, 2 starting from 1st April to 29th May 2020.

is depicted in Figure 5.

This situation arises as we increase α_2, then the government quarantined technique is slackly applied to the population. In this case $\alpha_2 = 3 \times 10^{-10}$, the pick of infection reached almost 125 days after 1st April 2020, and the total number of highest infected individuals will be around 3000000.

Also, we making $\alpha_1 = \alpha_2 = 2 \times 10^{-10}$, i.e.,

if Government take a policy to convert all home quarantined individuals into government quarantined. In that case, the value of $R_0 = 1.6368 < 3.0909$ is less than the previous value of R_0. Therefore, infected individuals are automatic decreases, which are depicted in Figure 6.

Figure 6 shows that if the Government takes said policy, then the maximum number of infected is
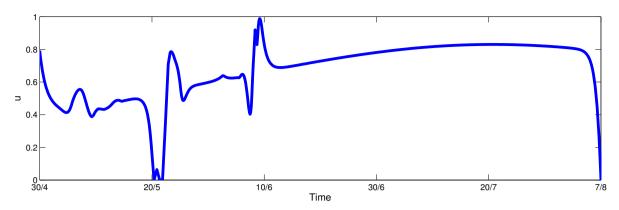
Fig. 7. The graph of u with respect to time t based on Table 1, 2 and $G_1 = 0.005$ and $G_2 = 1000$ starting from $30/4/2020$ to $7/8/2020$
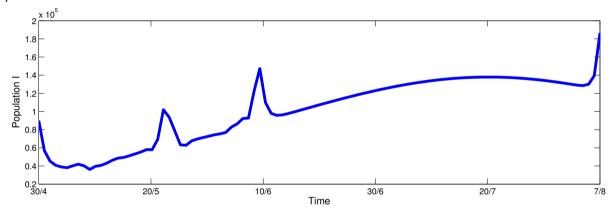

Fig. 8. The control diagram for the infected population (I) using data given in Table 1 along with $G_1 = 0.005$ and $G_2 = 1000$ from $30/4/2020$ to $7/8/2020$

restricted to about 8000. Unfortunately, to arrange this type of quarantined system is not possible for Government since India is a country with large populations. Therefore, the Government has to think above other possible ways to restrict Covid-19 infection.

Therefore, this paper provides a way to restrict the infection by optimal control policy. We try to recover the infected patients by using the minimum drug. The present section explores the idea to solve the control problem numerically and will interpret the findings graphically. The boundary value problem in this paper estranged boundary conditions ranges between $t = 0$ to $t = t_f$. The optimality problem is solved intended for 100 days. Actually, given time $t_f = 100$ represent the period at which the given treatment is stopped.

TABLE III
INITIAL DENSITIES FOR THE OPTIMAL CONTROL PROBLEM (17)

$S(0)$	$E(0)$	$H(0)$	$G(0)$	$I(0)$	$R(0)$
11.76×10^8	2×10^6	5×10^6	5×10^5	89987	16×10^6

The collocation method is the best technique to solve two-point BVPs numerically. The current optimization problem solves numerically using MATLAB for our control problem based on Table 1 and Table 3.

Here, we choose weight constants $G_1 = 0.005$ and $G_2 = 1000$, respectively in the objective function given in (17). Figure 7 represents the optimal control graphs for treatment control u. It shows that treatment control is very much necessary when the disease prevails. Also, this control function minimizes the cost function J.
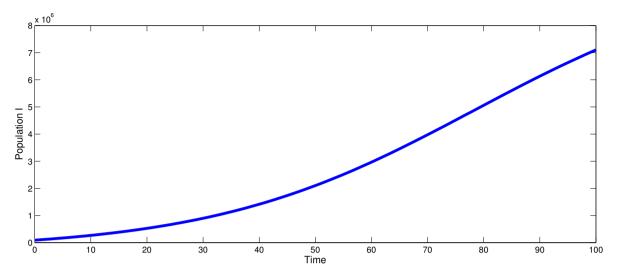
Fig. 9. Diagram for the infected populace (I) without control using data from Tables 1, 2 and $G_1 = 0.005$, $G_2 = 1000$ from $30/4/2020$ to $7/8/2020$
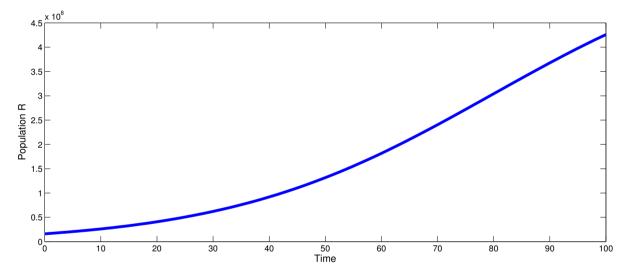

Fig. 10. The control diagram of the recovered population (R) based on Tables 1, 2 and $G_1 = 0.005$, $G_2 = 1000$ from $30/4/2020$ to $7/8/2020$

The graphs of the infected population (I) and recovered population (R) with treatment control and without treatment control with respect to time t are presented in Figure 8 to Figure 11, respectively.

From these figures, we can predict that treatment control is exceptionally efficient in reducing COVID infection. Therefore, control acquiesces the best result to control the Covid-19 epidemic outbreak.

VIII. DISCUSSIONS AND CONCLUSIONS

This paper explores the idea of a six-compartmental Covid-19 infection model fitted for the India scenario. The present model has exhibited the effects of different precautions proposed by the administration to control India's infectious disease. This study has also presented the impact of home and Government quarantined technique
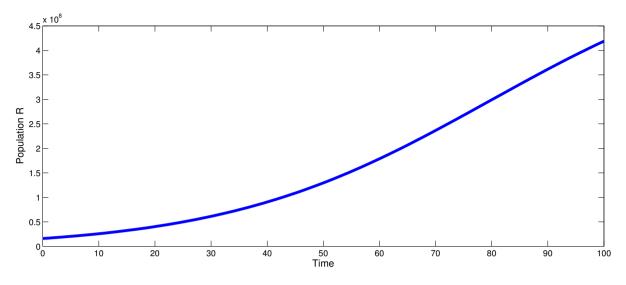
Fig. 11. Diagram of the recovered population (R) without of control based on Table 1, 2 and $G_1 = 0.005$, $G_2 = 1000$ during 30th April to 7th August 2020

on the Covid-19 epidemiological model via a non-linear differential equation system. The dynamical behavior of our proposed model is presented at DFE and endemic equilibrium points. We have calculated the BNR and verify that it behaves a crucial role in predicting the stability nature of all possible equilibrium points and the existence of the disease soon. Also, a sensitivity analysis of R_0 is carried out to α_1 and α_2 through Figure 2. This analysis has shown that the parameters α_1 and α_2 are vital to restrict the spread of infection.

The most crucial part related to public health importance is that this paper has built up a suitable optimal control problem to reduce the number of infected individuals. Though the infection may be controlled by reducing the parameters' values α_1 and α_2, it is not a long term solution to restrict the spread of the disease. Therefore, we deem the treatment of infected individuals by medicine as a control to diminish the spread of Covid-19 infection. In this paper, we include a quadratic control to quantify this goal. To minimize the objective functional (9), the control function $u(t)$ is considered.

This study also numerically verified the theoretical analysis by using MATLAB software to validate scientific findings through plot comparative figures of infected populations with different values of α_1 and α_2. We have observed from Figure 4 for $\alpha_1 = 2 \times 10^{-10}$ and $\alpha_1 = 1 \times 10^{-10}$ that the pick of infection will be attained in the mid of September 2020 and around 1700000 may be affected in that time. Again if the administration has taken the policy to cover all the populations under the Government quarantined process (which is impossible for a country like India), i.e., $\alpha_1 = \alpha_2$, then Figure 6 show that a maximum number of infected individuals are around 80000, the infection may be eradicated within October 2020.

The proposed optimal control strategies are beneficial to reduce the number of infected populations, which is presented through comparative Figure 8 to Figure 11. It may also be concluded from these figures that the only treatment of an infected individual by medicine may not be the possible way to die out the disease from India and the globe. Therefore, vaccination should be necessary as early as possible to protect the world from the Covid-19 endemic.

Our mathematical model on the Covid-19 epidemic diseases gives some consequences of public health policies. Many of our proposed model

parameters are assumed or estimated, but it depends on many factors; these parameters may be considered as fuzzy or stochastic rather than deterministic. Consequently, it may include fuzzy or stochastic differential equations in the proposed model for future work consideration. The progress of treating Covid-19 disease by different medicines in a cost-effective way is the main objective of health administrators, policy-makers, and scientists until a vaccine is discovered. The present paper gives a little effort to reach this objective to restrict Covid-19 infection.

REFERENCES

[1] S. E. Adler, Why Coronaviruses Hit Older Adults Hardest, AARP2020.

[2] J. Cohen, D. Normile, New SARS-like virus in China triggers alarm, Science 367 (6475) (2020) 234–235.

[3] P. Wang, X. Zheng, J. Li, B. Zhu, Prediction of epidemic trends in COVID-19 with logistic model and machine learning technics, Chaos Soliton Fract., 139 (2020), 110058.

[4] C. Pai, A. Bhaskar, V. Rawoot, Investigating the dynamics of COVID-19 pandemic in India under lockdown, Chaos Soliton Fract., 138 (2020), 109988.

[5] S. Djilali, B. Ghanbari, Coronavirus pandemic: A predictive analysis of the peak outbreak epidemic in South Africa, Turkey, and Brazi, Chaos Soliton Fract., 138 (2020), 109971.

[6] K. Ayinde, A. F. Lukman, R. I. Rauf, O. O. Alabi, C. E. Okon, O. E. Ayinde, Modeling Nigerian Covid-19 cases: A comparative analysis of models and estimators, Chaos Soliton Fract., 138 (2020), 109911.

[7] M. Yousaf, S. Zahir, M. Riaz, S. M. Hussain, K. Shah, Statistical analysis of forecasting COVID-19 for upcoming month in Pakistan, Chaos Soliton Fract., 138 (2020), 109926.

[8] I. Kırbaş, A. Sözen, A. D. Tuncer, F. Ş. Kazancıoğlu, Comparative analysis and forecasting of COVID-19 cases in various European countries with ARIMA, NARNN and LSTM approaches, Chaos Soliton Fract., 138 (2020), 110015.

[9] W. E. Alnaser, M. Abdel-Aty, O. Al-Ubaydli, Mathematical prospective of coronavirus infections in bahrain, saudi arabia and egypt, Inf. Sci. Lett., 09 (2020), 51-64.

[10] C. M. Păcurar, B. R. Necula, An analysis of COVID-19 spread based on fractal interpolation and fractal dimension, Chaos Soliton Fract., 139 (2020), 110073.

[11] P. Arora, H. Kumar, B. K. Panigrahi, Prediction and analysis of COVID-19 positive cases using deep learning models: A descriptive case study of India, Chaos Soliton Fract., 139 (2020), 110017.

[12] India covid-19 tracker. https://www.covid19india.org/, 2020. [Retrieved: 08/05/2020]

[13] Q. Pan, T. Gao, M. He, Influence of isolation measures for patients with mild symptoms on the spread of COVID-19, Chaos Soliton Fract., 139 (2020), 110022.

[14] B. K. Sahoo, B. K. Sapra, A data driven epidemic model to analyse the lockdown effect and predict the course of COVID-19 progress in India, Chaos Soliton Fract., 139 (2020), 110034.

[15] H. Panwar, P. K. Gupta, M. K. Siddiqui, R. Morales-Menendez, V. Singh, Application of deep learning for fast detection of COVID-19 in X-Rays using nCOVnet, Chaos Soliton Fract., 138 (2020), 109944.

[16] Y. Huang, Y. Wu, W. Zhang, Comprehensive identification and isolation policies have effectively suppressed the spread of COVID-19, Chaos Soliton Fract., 139 (2020), 110041.

[17] P. C. L. Silva, P. V. C. Batista, H. S. Lima, M. A. Alves, F. G. Guimarães, R. C. P. Silva, An agent-based model of COVID-19 epidemic to simulate health and economic effects of social distancing interventions, Chaos Soliton Fract., 139 (2020), 110088.

[18] B. K. Mishra, A. K. Keshri, Y. S. Rao, B. K. Mishra, B. Mahato, S. Ayesha, B. P. Rukhaiyyar, D. K. Saini, A. K. Singh, COVID-19 created chaos across the globe: Three novel quarantine epidemic models, Chaos Soliton Fract., 138 (2020), 109928.

[19] V. M. Marquioni, M. A. M. de Aguiar, Quantifying the effects of quarantine using an IBM SEIR model on scalefree networks, Chaos Soliton Fract., 138 (2020), 109999.

[20] H. B. Fredj, F. Chérif, Novel Corona virus disease infection in Tunisia: Mathematical model and the impact of the quarantine strategy, Chaos Soliton Fract., 138 (2020), 109969.

[21] N. Ferguson, D. Laydon, G. N. Gilani, N. Imai, K. Ainslie, M. Baguelin, S. Bhatia, A. Boonyasiri, Z. C. Perez, G. Cuomo-Dannenburg, et al. Report 9: Impact of non-pharmaceutical interventions (npis) to reduce covid19 mortality and healthcare demand. 2020.

[22] B. Tang, N. L. Bragazzi, Q. Li, S. Tang, Y. Xiao, J. Wu, An updated estimation of the risk of transmission of the novel coronavirus (2019-ncov). Infectious Disease Modelling, 5 (2020) 248-255.

[23] R. Anguelov, J. Banasiak, C. Bright, J. Lubuma, R. Ouifki, The big unknown: The asymptomatic spread of COVID-19, Biomath. 9 (2020), 2005103.

[24] A. Behnood, E. Mohammadi Golafshani, S. M. Hosseini, Determinants of the infection rate of the COVID-19 in the U.S. using ANFIS and virus optimization algorithm (VOA), Chaos Soliton Fract., 139 (2020), 110051.

[25] R. G. da Silva, M. H. D. M. Ribeiro , V. C. Mariani,

L. D. S. Coelho, Forecasting Brazilian and American COVID-19 cases based on artificial intelligence coupled with climatic exogenous variables, Chaos Soliton Fract., 139 (2020), 110027.

[26] P. C. L. Silva, P. V. C Batista, H. S. Lima, M. A. Alves, F. G. Guimarães, R. C. P. Silva, An agent-based model of COVID-19 epidemic to simulate health and economic effects of social distancing interventions, Chaos Soliton Fract., 139 (2020), 110088.

[27] D. Okuonghae, A. Omame, Analysis of a mathematical model for COVID-19 population dynamics in Lagos, Nigeria, Chaos Soliton Fract., 139 (2020), 110032.

[28] B. J. Quilty, S. Cliord, et al. Effectiveness of airport screening at detecting travellers infected with novel coronavirus (2019-ncov), Eurosurveillance, 25(5) (2020).

[29] M. Shen, Z. Peng, Y. Xiao, L. Zhang, Modelling the epidemic trend of the 2019 novel coronavirus outbreak in china. bioRxiv, 2020.

[30] B. Tang, X. Wang, Q. Li, N. L. Bragazzi, S. Tang, Y. Xiao, J. Wu, Estimation of the transmission risk of the 2019-ncov and its implication for public health interventions. Journal of Clinical Medicine, 9(2) (2020) 462.

[31] V. Soukhovolsky, A. Kovalev, A. Pitt, B. Kessel, A new modelling of the COVID 19 pandemic, Chaos Soliton Fract., 139 (2020), 110039.

[32] Sk S. Nadim, I. Ghosh, J. Chattopadhyay, Short-term predictions and prevention strategies for covid-2019: A model based study. arXiv preprint arXiv:2003.08150, 2020.

[33] M. Cadoni, G. Gaeta, Size and timescale of epidemics in the SIR framework, Physica D, 411 (2020), 132626.

[34] Y. Zhang, X. Yu, H. Sun, G. R. Tick, W. Wei, B. Jin, Applicability of time fractional derivative models for simulating the dynamics and mitigation scenarios of COVID-19, Chaos Soliton Fract., 138 (2020), 109959.

[35] M. Higazy, Novel fractional order SIDARTHE mathematical model of COVID-19 pandemic, Chaos Soliton Fract., 138 (2020), 110007.

[36] J. T. Wu, K. Leung, G. M Leung, Nowcasting and forecasting the potential domestic and international spread of the 2019-ncov outbreak originating in wuhan, china: a modelling study. The Lancet, 395(10225) (2020) 689-697.

[37] J. M. Read, J. RE Bridgen, D. AT Cummings, A. Ho, C. P Jewell, Novel coronavirus 2019-ncov: early estimation of epidemiological parameters and epidemic predictions, MedRxiv, 2020.

[38] A. Paul, S. Chatterjee, N. Bairagi, Prediction on Covid-19 epidemic for different countries: Focusing on South Asia under various precautionary measures, medRxiv, 2020.

[39] T. Sardar, Sk S. Nadimb, J. Chattopadhyayb, Assessment of 21 days lockdown effect in some states and overall India: A predictive mathematical study on COVID-19 outbreak, arXiv preprint arXiv:2004.03487V1, 2020.

[40] D. Pal, D. Ghosh, P.K. Santra, G.S. Mahapatra, Mathematical analysis of a COVID-19 epidemic model by using data driven epidemiological parameters of diseases spread in India, medRxiv, 2020.

[41] P. Van den Driessche, J. Watmough, Reproduction numbers and sub-threshold endemic equilibria for compartmental models of disease transmission, Math Biosci 180 (2002) 29–48.

[42] S. Çakan, Dynamic analysis of a mathematical model with health care capacity for COVID-19 pandemic, Chaos Soliton Fract., 139 (2020), 110033.

[43] K. Y. Ng, M. M. Gui, COVID-19: Development of a robust mathematical model and simulation package with consideration for ageing population and time delay for control action and resusceptibility, Physica D, 411 (2020), 132599.

[44] N. Al-Asuoad, S. Alaswad, L. Rong, M. Shillor, Mathematical model and simulations of MERS outbreak: Predictions and implications for control measures, Biomath 5 (2016), 1612141

[45] H. Zhao, Z. Feng, Staggered release policies for COVID-19 control: Costs and benefits of relaxing restrictions by age and risk, Chaos Soliton Fract., 138 (2020), 108405.

[46] Z. Abbasi, I. Zamani, A. H. A. Mehra, M. Shafieirad, A. Ibeas, Optimal Control Design of Impulsive SQEIAR Epidemic Models with Application to COVID-19, Chaos Soliton Fract., 139 (2020), 110054.

[47] V. Mbazumutima, C. Thron, L. Todjihounde, E. numerical solution for optimal control using treatment and vaccination for an SIS epidemic model, Biomath 8 (2019), 1912137.

[48] S. Lenhart, J. T. Workman, Optimal control applied to biological models. Mathematical and computational biology. Boca Raton (Fla.), London: Chapman & Hall/CRC, 2007.

[49] A. C. Chiang, Elements of dynamic optimization. New York, NY: McGraw-Hill international editions, McGraw-Hill. [u.a.], internat. ed. edition, 1992.

[50] R. M. Anderson, R. M. May, Population biology of infectious diseases. Part I, Nature, 280 (1979) 361–367.

[51] F. Brauer, C. Castillo-Chavez, Mathematical Models in Population Biology and Epidemiology (Springer, Berlin, 2001).

[52] A. Vivas-Barber, C. Castillo-Chavez, E. Barany, Dynamics of an "SAIQR" Influenza Model, Biomath 3 (2014), 1409251

[53] F. Nyabadza, S. D. Hove-Musekwa, From heroin epidemics to methamphetamine epidemics: Modeling substance abuse in a South African province, Math. Biosci. 225 (2010) 132–140.

[54] P. van den Driessche, J. Watmough, Reproduction numbers and sub-threshold endemic equilibria for compartmental models of disease transmission, Math. Biosci. 180 (2002) 29–48.

[55] Carlos Castillo-Chavez, Zhilan Feng, Wenzhang Huang, On the computation of R_0 and its role on Global Stability, Mathematical approaches for emerging and reemerging infectious diseases: an introduction, 1:229, 2002.

[56] K. Blayneh, Y. Cao, H. D. Kwon, Optimal control of vectorborne disease: treatment and prevention, Discrete Continuous Dyn. Syst. Ser. B 11 (2009) 1–31.

[57] C. Castillo-Chevez, Z. Feng, Global stability of an agestructure model for TB and its applications to optimal vaccination strategies, Math Biosci 151(1998) 135–154.

[58] D. T. Fleming, J. N. Wasserheit, From epidemiological synergy to public health policy and practice: the contribution of other sexually transmitted diseases to sexual transmission of HIV infection, Sex Transm. Infect. 75(4) (1999) 3–17.

[59] H. R. Joshi, Optimal control of an HIV immunology model, Optim. Control. Appl. Methods 23 (2002) 199–213.

[60] L. S. Pontryagin, V. G. Boltyanskii, R. V. Gamkrelidze, E. F. Mishchenko, The mathematical theory of optimal processes. Gordon and Breach Science, London, 1986.

[61] knoema, https://knoema.com/atlas/India/Birth-rate, Retrieved : 2020-04-08.

[62] M. Kot, Elements of Mathematical Ecology, Cambridge University Press, Cambridge, 2001.

Appendix A. Proof of Theorem 4

The variational matrix of system (3) at DFE E_0 is given by

$$
M_{E_0} = \begin{bmatrix}
-d_1 & 0 & -\frac{\alpha_1\Lambda}{d_1} & -\frac{\alpha_2\Lambda}{d_1} & 0 & 0 \\
0 & -A & \frac{\alpha_1\Lambda}{d_1} & \frac{\alpha_2\Lambda}{d_1} & 0 & 0 \\
0 & \beta_1 & -B & 0 & 0 & 0 \\
0 & \beta_3 & 0 & -C & 0 & 0 \\
0 & \beta_2 & \gamma_2 & \sigma_2 & -D & 0 \\
0 & 0 & \gamma_1 & \sigma_1 & \in & -d_1
\end{bmatrix}
$$

Therefore, eigenvalues of the characteristic equation of M_{E_0} are $-d_1, -d_1$ and $-D$ and and the solution of the cubic equation,

$$P(\lambda) \equiv \lambda^3 + A_1\lambda^2 + A_2\lambda + A_3 = 0 \quad \text{(A.1)}$$

where

$$
\begin{aligned}
A_1 &= (A + B + C), \\
A_2 &= (AB + AC)(1 - R_0) + BC \\
&\quad + \left(\frac{\alpha_1\beta_1 C}{B} + \frac{\alpha_2\beta_3 B}{C}\right)\frac{\Lambda}{d_1}, \\
A_3 &= ABC(1 - R_0).
\end{aligned}
$$

Now, it is easily noted that, $A_1 > 0$, $A_3 > 0$ if $R_0 < 1$. After some simplifications, we get

$$
\begin{aligned}
A_1 A_2 - A_3 &= (A + B)AB\left[(1 - R_0) + \frac{\Lambda\alpha_2\beta_3}{d_1 AC}\right] \\
&\quad + (A + C)AC\left[(1 - R_0) + \frac{\Lambda\alpha_1\beta_1}{d_1 AB}\right] \\
&\quad + BC(B + C) + 2ABC
\end{aligned}
$$

Here, we can notice that, if $R_0 < 1$ then $A_1 A_2 - A_3 > 0$ if $R_0 < 1$. Therefore, by the Routh–Hurwitz Routh–Hurwitz criterion [62] it follows that $P(\lambda) = 0$ has negative real roots if $R_0 < 1$, i.e., the system (3) at DFE E_0 when $R_0 < 1$. This completes the proof.

Appendix B. Proof of Theorem 6

The variational matrix of system (3) at $E_1(S^*, E^*, H^*, G^*, I^*, R^*)$ is given by,

$$
M_{E_1} = \begin{bmatrix}
b_{11} & 0 & b_{13} & b_{14} & 0 & 0 \\
b_{21} & b_{22} & b_{23} & b_{24} & 0 & 0 \\
0 & b_{32} & b_{33} & 0 & 0 & 0 \\
0 & b_{42} & 0 & b_{44} & 0 & 0 \\
0 & b_{52} & b_{53} & b_{54} & b_{55} & 0 \\
0 & 0 & b_{63} & b_{64} & b_{65} & b_{66}
\end{bmatrix}
$$

where, $b_{11} = -d_1 R_0$, $b_{13} = -\alpha_1 S^*$, $b_{14} = -\alpha_2 S^*$, $b_{21} = d_1(R_0 - 1)$, $b_{22} = -A$, $b_{23} = \alpha_1 S^*$, $b_{24} = \alpha_2 S^*$, $b_{32} = \beta_1$, $b_{33} = -B$, $b_{42} = \beta_3$, $b_{44} = -C$, $b_{52} = \beta_2$, $b_{53} = \gamma_2$, $b_{54} = \sigma_2$, $b_{55} = -D$, $b_{63} = \gamma_1$, $b_{64} = \sigma_1$, $b_{65} = \in$, $b_{66} = -d_1$.

Therefore, eigenvalues of the characteristic equation of M_{E_1} are $-D$, $-d_1$ and the solution of the equation,

$$Q(\lambda) \equiv \lambda^4 + B_1\lambda^3 + B_2\lambda^2 + B_3\lambda + B_4 = 0 \quad \text{(B.1)}$$

where

$$
\begin{aligned}
B_1 &= A + B + C + d_1 R_0, \\
B_2 &= \frac{\Lambda}{d_1 R_0}\left[\frac{\alpha_1\beta_1 C}{B} + \frac{\alpha_2\beta_3 B}{C}\right] \\
&\quad + (A + B + C)d_1 R_0 + BC, \\
B_3 &= (\alpha_1\beta_1 + \alpha_2\beta_3)d_1(R_0 - 1) + BCd_1 R_0 \\
&\quad + \frac{\Lambda\alpha_1\beta_1 C}{B} + \frac{\Lambda\alpha_2\beta_3 B}{C} \\
B_4 &= ABCd_1(R_0 - 1).
\end{aligned}
$$

Now, it is easily noted that $B_i > 0$ $(i = 1, 2, 3)$ and $B_4 > 0$ if $R_0 > 1$.

By the Routh–Hurwitz criterion [62], it follows that $Q(\lambda) = 0$ has negative real roots if

$B_i > 0$ for $i = 1, 2, 3, 4$,

$D_1 = B_1 > 0$,

$D_2 = \begin{vmatrix} B_1 & B_3 \\ 1 & B_2 \end{vmatrix} = B_1 B_2 - B_3 > 0$,

$$D_3 = \begin{vmatrix} B_1 & B_3 & 0 \\ 1 & B_2 & B_4 \\ 0 & B_1 & B_3 \end{vmatrix}$$
$$= B_1 B_2 B_3 - B_1^2 B_4 - B_3^2 > 0.$$

Therefore the system (3) shows local asymptotic stability at E_1 when $R_0 > 1$, $B_1 B_2 - B_3 > 0$ and $B_1 B_2 B_3 - B_1^2 B_4 - B_3^2 > 0$. This completes the proof.